4681 (RP-1168)

Exhaust Contamination of Hidden vs. Visible Air Intakes

Ronald L. Petersen, Ph.D.
Member ASHRAE

John J. Carter
Member ASHRAE

John W. LeCompte
Associate Member ASHRAE

ABSTRACT

A wind tunnel dispersion modeling study was conducted to investigate exhaust contamination of hidden versus visible air intakes. A "hidden" intake is typically on a building sidewall or on the sidewall of a roof obstruction opposite the exhaust source. A "visible" intake is at roof level or on top of an obstruction, directly above the hidden intake. Overall, the study has shown what designers suspected: placing air intakes on building sidewalls is beneficial when the stacks are on the roof. Significant concentration reductions were found when air intakes are placed right below the building roof edge on the building sidewall. The farther down the building sidewall the air intake is placed, the larger the reduction. However, the largest relative reduction between a visible and hidden intake is achieved by just moving the intake a few feet from the edge of the building roof to a point just around the corner on the building sidewall.

INTRODUCTION

This paper documents ASHRAE Research Project 1168-TRP on exhaust contamination of hidden versus visible air intakes. Throughout this paper, a hidden intake is typically on a building sidewall or roof obstruction sidewall, while a visible intake is at roof level or on top of an obstruction, directly above the hidden intake. Designers commonly place air intakes on the walls of the building, just below the roof in the belief that these hidden intakes will have less contamination from roof-mounted exhaust sources than if the intakes are on the roof itself. This paper provides documentation supporting this design practice and also provides methods to quantify the level of concentration reduction that is achieved when intakes are hidden.

The specified objective of this research was to compare the effects on exhaust-to-intake concentration reduction (dilution) for hidden versus visible air intake locations and to produce a set of design guidelines and a concentration (dilution) calculation procedure suitable for inclusion in the *ASHRAE Handbook—HVAC Applications*. To meet the project objectives, three major tasks were conducted: (1) a literature review of experimental data concerning the concentration reductions achieved at hidden intakes relative to the visible intakes; (2) an experimental program using scale models of three representative buildings in a boundary layer wind tunnel to study the effects of exhaust configurations, meteorological conditions, building configurations, and hidden versus visible intake configurations on concentration, velocity, and turbulence; and (3) analysis of the data to identify key variables and to develop a simple method to predict concentration reductions at hidden intakes. General design guidelines regarding hidden intakes were also developed as part of task three.

BACKGROUND INFORMATION

The literature review revealed a wealth of research regarding concentration predictions and observations at visible intakes. Several studies of concentrations in building wakes (Huber 1978, 1988a, 1988b, 1989) as well as a few studies of clusters of buildings (Wilson et al. 1998; Hosker 1985) were identified. Six studies that specifically tested hidden air intake locations on buildings of simple geometry are discussed below (Halitsky 1963; Wilson 1976, 1977a, 1977b; Li and Meroney 1983; Petersen et al. 1997).

Each of the six studies added specific detail for understanding the variables relevant to concentration predictions at

Ronald L. Petersen is vice president and **John J. Carter** is a senior project engineer at Cermak Peterka Petersen, Inc., Fort Collins, Colo. **John W. LeCompte** is a graduate student at Colorado State University, Fort Collins, Colo.

air intakes. The effects of exhaust momentum, stack height, wind direction, stack location, and architectural screens were examined. Most of the studies based their predictions on stretched-string distance, S, velocity ratio, V_e/U_h, and exit area, A_e, but did not differentiate between hidden and visible intakes. Therefore, no beneficial effect was predicted when the intake was moved from the top of the roof edge to the top of the building sidewall. Only Li and Meroney (1983) suggested a different distance dilution parameter, B_1, for hidden air intakes versus visible intakes (according to ASHRAE [1999], Chapter 43, but not stated outright in the published article). There are even conflicting conclusions between two of the studies. Wilson (1976) concluded that using a hidden air intake has no benefit in reducing concentrations, while Li and Meroney (1983) concluded that there is a significant benefit. Three of the studies (Wilson 1976, 1977b; Li and Meroney 1983) were performed with very low exhaust velocities in order to simulate capped stacks or leaks and were not intended for use in the design of exhausts with significant exit velocities. Halitsky (1963) utilized a uniform mean approach velocity with negligible turbulence, which would not accurately represent the atmospheric boundary layer. Despite the value of this research, the results from all of these studies were disqualified for inclusion in this analysis for either of the following reasons: the velocity ratio was not varied through a range in order to find the critical maximum concentration at the roof edge and at the hidden receptor, or only cases with insignificant plume rise were investigated.

Petersen et al. (1997) investigated the influence of architectural screens on exhaust dilution at visible and hidden air intakes. One building was studied with three exhaust velocities and two wind speeds. The visible and hidden intake concentration data were considered for inclusion in this study but were disqualified since the overall maximum concentrations on the roof and sidewall were not determined. The results from Petersen et al. (1997) were used to provide a rough check on the general equation that was developed as part of this study.

Overall, the literature review provided information such that representative building geometries could be identified for this evaluation and provided further justification for this research.

WIND TUNNEL DATABASE

Wind Tunnel Simulation of Airflow and Dispersion

An accurate simulation of the boundary-layer winds and stack gas flow is an essential prerequisite to any wind tunnel study of diffusion around buildings. The similarity requirements can be obtained from dimensional arguments derived from the equations governing fluid motion. A detailed discussion of these requirements is given in Snyder (1981). The criteria and experimental methods that were used for conducting the wind tunnel simulations are discussed in detail in Petersen and LeCompte (2002). Since this study was designed to be generic in nature, rectangular buildings were placed in one of two uniform roughness configurations. The roughness configurations were designed to simulate either a rural environment with a surface roughness length of 0.30 m or an urban environment with a surface roughness length of 0.80 m.

General Description of Test Plan

Concentration and velocity measurements were obtained on 1:100 scale models for three different building geometries with various exhaust stack configurations and meteorological conditions. The building geometries were determined by reviewing typical laboratory and commercial building shapes (Petersen and LeCompte 2002). Table 1 summarizes the dimensions of the buildings evaluated for this study and the building used by Petersen et al. (1997). Figure 1 is an isometric drawing of Building 1, a large flat-roofed, low-rise structure representative of a shopping center or commercial plant. For selected tests, a long or short barrier at one of two locations downwind from the stack was installed, as shown in Figure 1. Most testing was conducted with a flat, unobstructed roof.

Concentrations were measured at hidden and visible intakes for a range of exhaust stack heights, volume flow rates, and wind speeds at each of three wind directions: normal to the short side, normal to the long side, and diagonal. Stack locations were designated S1 through S7, and receptor locations were designated R1 through R17, as shown in Figure 1. Using the criteria described in Petersen and LeCompte (2002) and source characteristics specified in Table 2, the model test

Table 1. Physical Characteristics of Buildings Evaluated

Building Number	Height ft (m)	Length ft (m)	Width ft (m)	Number of Floors	Total Area ft² (m²)	L/H	W/H	Comment
1	30 (9.1)	150 (45.7)	90 (27.4)	2	27,000 (2509.7)	5.0	3.0	
2	75 (22.9)	300 (91.5)	150 (45.7)	5	225,000 (20,913.9)	4.0	2.0	
3	150 (45.7)	375 (114.3)	75 (22.9)	10	281,250 (26,142.4)	2.5	0.5	
4	50 (15.2)	100 (30.5)	50 (15.2)	3	15,000 (1394.3)	2.0	1.0	Test Building For ASHRAE 805-TRP

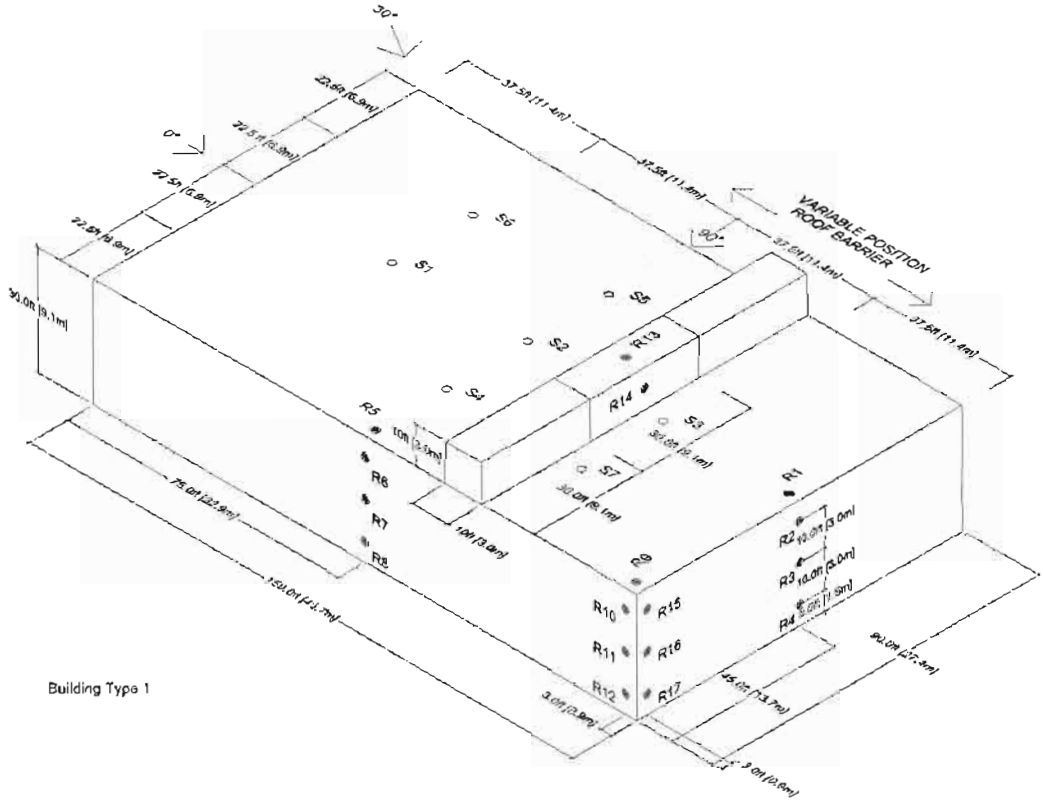

Figure 1 *Building dimensions with stack and receptor locations for Building 1—large, flat-roofed, low-rise shopping center or commercial plant.*

Table 2. Full-Scale Exhaust Parameters

Source Description	Exit Diameter, d in. (m)	Volume Flow Rate, Q cfm (m^3/s)	Exit Velocity, V_e fpm (m/s)
Low Flow	6.8 (0.17)	500 (0.24)	2000 (10.2)
Medium Flow	21.4 (0.54)	5000 (2.36)	2000 (10.2)
High Flow	67.7 (1.72)	50000 (23.6)	2000 (10.2)

conditions were computed for three generic stack configurations designated low flow (500 cfm, 0.24 m^3/s), medium flow (5000 cfm, 2.36 m^3/s), and high flow (50,000 cfm, 23.6 m^3/s). All stacks were tested in the rural environment for each building. Only the medium flow stack was tested in the urban environment for each building. A full range of anemometer wind speeds (1 to 20 m/s, 2.24 to 44.7 mph) was tested in order to determine the highest concentrations achievable at the roof and sidewall receptors. Detailed information on the wind tunnel, instrumentation, and boundary layer documentation can be found in Petersen and LeCompte (2002).

Mean velocity and longitudinal, lateral, and vertical turbulence intensity were measured in the rural roughness configuration at heights corresponding to 5, 10, 15, 20, 30, and 40 ft (1.52, 3.05, 4.57, 6.10, 9.15, and 12.2 m) above each stack location for each wind direction. Velocity measurements using the urban approach roughness were only obtained for Building 2. The purpose of these measurements was to determine how the building altered the approach flow and to develop inputs for the dispersion models. The results of these measurements are described in Petersen and LeCompte (2002).

ANALYTICAL METHODS

General

Existing analytical methods were used as the starting point for developing and evaluating the method for estimating concentrations at visible and hidden air intakes. Chapter 43 of the *1999 ASHRAE Handbook—HVAC Applications* (ASHRAE 1999) describes a commonly used method for predicting the concentration at a visible intake. Another method is a basic Gaussian analysis (Turner 1994). Both of these methods, as well as an enhanced Gaussian analysis, are described briefly in this section.

Concentration Prediction—ASHRAE Method

In Chapter 43 of the *1999 ASHRAE Handbook—HVAC Applications* (ASHRAE 1999), the critical dilution (concentration) is first calculated for a flush vent (a stack with $h_s = 0$), then adjusted for the actual stack height under consideration. This method uses the following parameters: emission mass flow rate; stack height, exit area, and exit velocity; stretched string distance; and simplified terms to describe the plume spread.

Concentration Prediction—Standard Gaussian Method

The Gaussian plume model can be simplified to the following equation for a centerline receptor at the surface of a reflecting roof or at ground level:

$$\frac{C}{m} = \frac{1 \times 10^6}{\pi U_h \sigma_y \sigma_z} \exp\left[-\frac{1}{2}\left(\frac{h_s + \Delta h_T}{\sigma_z}\right)^2\right] \quad (1)$$

where C is the pollutant concentration (μg/m^3); m is the pollutant mass emission rate (g/s); U_h is the mean wind speed at stack top (m/s); σ_y and σ_z are the standard deviations of plume concentration distribution in the crosswind and vertical directions at downwind distance x, respectively; h_s is the stack height above the roof, receptor, or ground level as appropriate; and Δh_T is the net effective rise of the plume centerline above the stack top.

For the standard method, the approach wind conditions at stack height are used rather than the local conditions at the stack top. This allows for straightforward calculations of U_h, σ_y, and σ_z. The mean wind speed is characterized by a power law relationship:

$$U_h = U_{anem}\left(\frac{z_\infty}{z_{anem}}\right)^{n_{anem}}\left(\frac{z_s}{z_\infty}\right)^{n_{site}} \quad (2)$$

where U_{anem} is the mean wind speed at the anemometer height, z_{anem}; z_∞ is the free stream height; n_{anem} is the power law exponent at the anemometer; z_s is the stack height above ground level; and n_{site} is the power law exponent at the building site. The power law exponents, n_{site} and n_{anem}, can be calculated based on surface roughness classification or can be determined empirically by a curve fit to a model-scale approach velocity profile.

The lateral and vertical plume dispersion coefficients, σ_y and σ_z, can be calculated using the empirical equations in the EPA AERMOD model (Cimorelli et al. 1998) and can be represented as a function of two factors,

$$\sigma_y = (\sigma_{y0}^2 + \sigma_{yt}^2)^{0.5} \quad \text{and} \quad \sigma_z = (\sigma_{z0}^2 + \sigma_{zt}^2)^{0.5}, \quad (3)$$

where σ_{y0} and σ_{z0} are initial lateral and vertical plume dispersion, and σ_{yt} and σ_{zt} are lateral and vertical plume dispersion due to ambient turbulence. According to Turner (1994),

$$\sigma_{y0} = \sigma_{z0} = 0.35d, \quad (4)$$

where d is the stack diameter. According to Cimorelli et al. (1998), the crosswind and vertical ambient turbulence dispersion coefficients, σ_{yt} and σ_{zt}, are calculated as linear functions of distance from the exhaust source, based on the longitudinal turbulence intensity at stack height in the approach wind.

$$\sigma_{yt} = I_{ys,ap}x = A_1 I_{xs,ap}x$$

and (5)

$$\sigma_{zt} = I_{zs,ap}x = A_2 I_{xs,ap}x,$$

where $I_{ys,ap}$ and $I_{zs,ap}$ are the lateral and vertical turbulence intensities in the approach flow at stack height, $I_{xs,ap}$ is the longitudinal turbulence intensity in the approach flow at stack height, A_1 and A_2 are empirical constants, and x is the downwind distance to the receptor location. For flat homogenous terrain, Snyder (1981) suggests the following values:

$$A_1 = 0.75 \quad \text{and} \quad A_2 = 0.50. \quad (6)$$

$I_{xs,ap}$ is determined by either an empirical relationship to height, heat transfer, mixing depth, temperature, gravity, and fluid properties (Cimorelli et al. 1998) or by a curve fit to an observed approach longitudinal turbulence intensity profile. For this study, $I_{x,ap}$ for the rural and urban approaches measured in the wind tunnel were found to agree with the following equations:

$$I_{x,ap} = 7.6692\left(\frac{z}{z_{ref}}\right)^{0.3631} - 7.5252\left(\frac{z}{z_{ref}}\right)^{0.3835} \text{(rural)} \quad (7)$$

$$I_{x,ap} = 7.6798\left(\frac{z}{z_{ref}}\right)^{0.3591} - 7.5121\left(\frac{z}{z_{ref}}\right)^{0.3849} \text{(urban)} \quad (8)$$

The second term was added after the first term alone failed to produce an adequate fit. The best-fit constants were found by minimizing the normalized root-mean-square error (RMSE) over the range of z values used in the study.

Net effective plume rise, Δh_T, was calculated using Briggs (1969, 1975) for a neutrally buoyant plume using the following equation:

$$\Delta h_T = \left(\frac{3F_m x}{\beta_j^2 U_h^2}\right)^{\frac{1}{3}} \quad (9)$$

where

x = downwind distance,
β_j = entrainment parameter, and
F_m = momentum flux, defined as

$$F_m = V_e^2 \frac{d_s^2}{4}\frac{T_a}{T_s}. \quad (10)$$

Concentration Prediction—Modified Gaussian Method

For short rooftop stacks, the presence of the building disturbs the flow, creating a significantly different set of mean velocity and turbulence conditions at the stack top than in the approach flow. In the approach flow, mean wind speed, $U_{h,ap}$, and longitudinal turbulence intensity, $I_{x,ap}$, can be readily characterized with confidence from established relationships using terrain classification. However, there are no simple means to calculate these values accurately in the disturbed region above the building. Also, the lateral and vertical ambient turbulence dispersion coefficients, σ_{yI} and σ_{zI}, are often based on turbulence intensities in the approach, $I_{ys,ap}$ and $I_{zs,ap}$, which are generally simplified as constant scalings of the approach longitudinal turbulence intensity, $I_{xs,ap}$, as discussed above. Therefore, Gaussian approaches to concentration and dilution predictions are often based on approach conditions, and concentration (dilution) predictions must account for the effect of the building elsewhere in the analysis.

Therefore, a modified Gaussian method is presented, which uses more accurate wind speed and turbulence values at the stack. Calculation of the mean wind speed at the stack top, U_h, is carried out by introducing an adjustment factor, $U_h / U_{h,ap}$, to account for the building's effect on the approach wind.

$$U_h = \left(\frac{U_h}{U_{h,ap}}\right) U_{h,ap} \tag{11}$$

where U_h is the stack top wind speed, $U_h/U_{h,ap}$ is the factor for a specific stack/building configuration that relates the approach wind speed to that at the stack location, and $U_{h,ap}$ is the mean approach wind speed at the stack height.

The crosswind and vertical ambient turbulence dispersion coefficients, σ_{yI} and σ_{zI}, are again calculated as linear functions of distance from the exhaust source based on the longitudinal turbulence intensity modified by an empirical term that corrects for the presence of the building.

$$\sigma_{yI} = (I_{ys}x) = \left[\left(\frac{I_y}{I_{x,ap}}\right)_s I_{xs,ap}x\right]$$

and (12)

$$\sigma_{zI} = (I_{zs}x) = \left[\left(\frac{I_z}{I_{x,ap}}\right)_s I_{xs,ap}x\right]$$

where $I_{xs,ap}$ is the longitudinal turbulence intensity at stack height in the approach flow, and $(I_y/I_{x,ap})_s$, $(I_z/I_{x,ap})_s$ are factors for a specific stack/building configuration that relate the approach longitudinal turbulence intensity to the lateral and vertical turbulence intensity at the stack location. For each building evaluated, the mean velocity and turbulence adjustment factors, $U_h/U_{h,ap}$, $(I_y/I_{x,ap})_s$, and $(I_z/I_{x,ap})_s$, were calculated based on the velocity measurements discussed in Petersen and LeCompte (2002).

RESULTS

Concentration reduction factors were computed from the wind tunnel concentration measurements and analyzed to determine general trends. General equations were then developed to predict concentration reduction factors between the visible and top hidden (sidewall) receptors, F_{VH}, and for receptors at various heights along the building sidewall, F_{SW}. Finally, a method to estimate sidewall concentrations for real building situations was developed. The method was tested against the wind tunnel database of visible and hidden concentration measurements.

Concentration Reduction Factors

Visible/Hidden Reduction Factors. A visible/hidden reduction factor, F_{VH}, is defined as the concentration at the downwind roof edge (i.e., visible receptor) divided by the concentration at the top sidewall (i.e., hidden) receptor. The top sidewall receptor was used because that location usually had the highest concentration and, therefore, the lowest uncertainty of the hidden receptors. Three key variables affecting F_{VH} were identified from analysis of the wind tunnel data: exhaust volume flow, normalized plan area (A_P), and normalized stack height. No general trend was found to describe the effect of stack location on F_{VH}. The important variables are defined as

$$\text{Exhaust Volume Flow} = V_e A_e = \frac{\pi V_e d^2}{4};$$

$$A_P = \frac{WL}{H_b^2}; \text{ and}$$

$$\text{Normalized Stack Height} = \frac{h_s}{R}.$$

In order to develop a general equation for F_{VH} as a function of the above variables, the concentration data were separated into low, medium, and high exhaust flow ranges. Only values from the center stack for Buildings 1, 2, and 3 in the suburban approach roughness configuration were used. The equations were evaluated later using all data sets, as discussed below. F_{VH} results with uncertainty greater than 25% (generally extremely low concentrations) were omitted to ensure the most reliable relationship was developed.

Inspection of the data indicated the following trends: the F_{VH} value tended to increase as A_P decreased, and the F_{VH} values tended to decrease, with a lower limit of $F_{VH} = 1$, as the normalized stack height increased. Therefore, the following equation form was chosen:

$$F_{VH} = A_1\left\{1 - \exp\left[-\left(\frac{WL}{H_b^2}\right)^{A_2}\right]\right\}\left\{A_3 - \exp\left[\left(\frac{h_s}{R}\right)^{A_4}\right]\right\} \tag{13}$$

The best fit constants, A_1, A_2, A_3, and A_4, for each exhaust volume flow range were determined by minimizing the RMS error (RMSE) between predicted and observed F_{VH} values.

Initial results showed higher predicted reduction factors for the high flow stack than for the medium flow stack. This result was not the expected trend from a theoretical standpoint due to the relative plume sizes and centerline heights and was likely the result of low concentration values (i.e., higher measurement error) on the building sidewall for the high flow stacks and the smaller data set for the high flow stack. More realistic predictions resulted from fitting the medium and high flow stacks at the same time. Combining these data sets resulted in a large data set with a lower percentage of points likely to have significant measurement error. As a result, the predicted reduction factors followed the expected trend. The final set of data fit constants for low flow and medium and high flow stacks are shown in the right two columns of Table 3. The final F_{VH} values computed from Equation 13 are presented in Table 4.

Figures 2a and 2b show the F_{VH} data for upwind and downwind stack locations, urban approach roughness, and Building 4 (Petersen et al. 1997), with the curve fits based on the suburban approach, center stack data for Buildings 1, 2, and 3. The additional data, excluding the Building 4 data, are bounded adequately by the fits based on the center stack, suburban approach data. In the Building 4 study (Petersen et al. 1997), concentrations were taken at only two full-scale anemometer wind speeds—either 5.52 or 16.6 mph (2.47 or 7.44 m/s)—so the overall maximum concentration on the roof and building sidewall was not determined. In the current study, a range of six anemometer wind speeds spanning 1 to 20 m/s (2.24 to 44.7 mph) was evaluated, ensuring that the overall maximum concentrations were determined. However, the results presented in Figures 2a and 2b suggest that the general relation developed for Buildings 1 through 3 applies for Building 4, as the F_{VH} values occur in the appropriate region.

The results show that concentration reductions for short buildings with short stacks ($h_s / R \leq 0.2$) will range from 2 to 5 depending upon the exhaust flow. For tall buildings with short stacks ($h_s / R \leq 0.06$), the reduction factors will range from 4 to 13, again depending upon exhaust flow. As the stack height increases relative to the building, the concentration reduction decreases and approaches one.

Sidewall Reduction Factors. The sidewall reduction factor, F_{SW}, is defined as the concentration at the top sidewall receptor divided by the concentration at the bottom sidewall receptor. This ratio was used as it provided for lower uncertainty than top- to mid-wall receptor data, as discussed in Petersen and LeCompte (2002). The variables affecting F_{SW} were determined to be stack height, h_s, and vertical distance from roof to receptor, Δz. A Gaussian concentration distribution from the plume centerline to the bottom of the sidewall was assumed in development of F_{SW} as follows:

$$F_{SW} = \left(\frac{C_{top}}{C_{bot}}\right) \propto \frac{\exp(A_5 h_s^2)}{\exp[A_5(h_s + \Delta z)^2]} \propto \exp[-A_5(\Delta z^2 + 2h_s\Delta z)] \tag{14}$$

where A_5 is a constant to account for enhanced vertical dispersion in the building wake. This relationship assumes constant horizontal and vertical dispersion coefficients and a constant wind speed as the plume transitions from the building roof to the sidewall.

The relationship $W^{A6}H^{A7}L^{A8}$ was initially considered to account for the for the effect of building shape on the wake dispersion, seeking optimum values for the constants Ai. When this analysis did not prove to collapse the data effectively, R^2 was considered and found to be more effective, where R is the ASHRAE (1999) scaling length defined as

$$R = B_s^{0.67} B_L^{0.33}, \tag{15}$$

where B_s is the smaller of the building upwind face height or width, and B_L is the larger dimension. The following general equation was assumed to fit the data

$$F_{SW} = \exp\left[-A_9\left(\frac{\Delta z^2 + 2h_s\Delta z}{1000m^2}\right)^{A_{10}}\left(\frac{R^2}{1m^2}\right)^{A_{11}}\right] \tag{16}$$

where the factors of 1000 m^2 and 1 m^2 are length scaling factors used to nondimensionalize the equation. The constants A_i were obtained by minimizing the RMS error between predicted and observed F_{SW}. Data with high uncertainties (i.e., low concentration values that have a significant experimental error), generally those points with $R > 118$ ft (36 m), were omitted to provide increased accuracy in the fit. A detailed discussion on the measurement accuracy is provided in Petersen and LeCompte (2002).

Table 3. Data Fit Constants for Visible/Hidden Reduction Factor Equation, F_{VH}

Best Fit F_{VH} Constants	Volume Flow			
	High	Medium	Low	High and Medium
A_1	13.89	12.61	20.00	11.90
A_2	-0.186	-0.117	-0.794	-0.092
A_3	1.65	2.69	2.19	2.65
A_4	0.926	0.089	-0.807	0.106
RMSE (%)	7.9	13.5	13.3	14.3

Table 4. Visible/Hidden Reduction Factors, F_{VH}, as a Function of Building Shape, Exhaust Flow Rate, and Stack Height for 0 and 90 Degree Wind Directions

Low Flow Stacks				
	Normalized Plan Area (WL/H_b^2)			
h_s/R	1.25	5	8	15
0.02	13.0	5.6	4.0	2.5
0.04	12.6	5.4	3.9	2.4
0.06	12.2	5.2	3.8	2.4
0.08	11.9	5.1	3.7	2.3
0.10	11.5	4.9	3.6	2.2
0.15	10.7	4.6	3.3	2.1
0.20	9.9	4.2	3.0	1.9
0.25	9.1	3.9	2.8	1.8
0.30	8.2	3.5	2.5	1.6
0.40	6.5	2.8	2.0	1.3
0.50	4.7	2.0	1.4	1.0
Medium and High Flow Stacks				
	Normalized Plan Area (WL/H_b^2)			
h_s/R	1.25	5	8	15
0.02	5.3	4.9	4.8	4.6
0.04	4.6	4.2	4.1	4.0
0.06	4.1	3.8	3.7	3.6
0.08	3.7	3.5	3.4	3.2
0.10	3.4	3.2	3.1	3.0
0.15	2.9	2.7	2.6	2.5
0.20	2.4	2.3	2.2	2.1
0.25	2.1	1.9	1.9	1.8
0.30	1.8	1.7	1.6	1.6
0.40	1.3	1.2	1.2	1.1
0.50	1.0	1.0	1.0	1.0

Note: The shaded areas represent data extrapolations or interpolations.

The constants in Equation 16 were developed for each of the three volume flows evaluated and for all flow rates combined. In general, the RMS error using all the data was only slightly worse than the RMS error when each volume flow was fitted individually. Hence, the fit constants for the collective set of data were used to develop charts that can be used to select a reduction factor for a particular building geometry. When either SI or I-P units are used, the constants are A_9 = 0.00172, A_{10} = 0.108, and A_{11} = 0.767. For I-P units, the 1000 m^2 and 1 m^2 constants must be converted to ft^2.

The equation developed for all flow cases was used to generate charts of F_{SW} versus R for various stack heights, as shown in Figure 3. The figure indicates only a slight difference between the predicted F_{SW} for no stack and that for the tallest stack (20 ft or 6.1 m). The difference was only 5.1% for the short building prediction, shown in the figure, and less for all taller building cases. Therefore, only the most conservative F_{SW} predictions (i.e., those for zero stack height) were used, as presented in Figures 4a and 4b for the bottom and mid-wall receptors, respectively. The figures show that as R approaches 0, F_{SW} approaches 1.0, and that as building height increases, F_{SW} increases up to the limit at R = 118 ft (36 m). Even though the trends in Figures 4a and 4b suggest F_{SW} will increase with increasing R, there was significant uncertainty in the experimental data with R > 118 ft (36 m). Therefore, when R > 118 ft (36 m), F_{SW} was limited to 1.0 to provide conservative results.

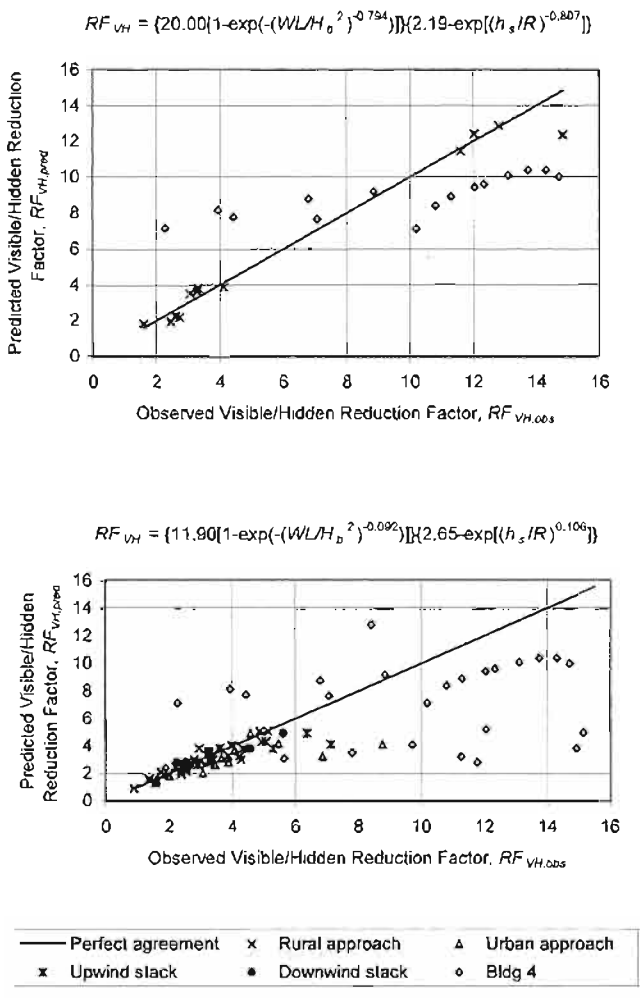

Figure 2 Predicted versus observed visible/hidden concentration reduction factors for 0 and 90 degree wind directions: (a) low flow center stacks, urban/rural approaches, all buildings; (b) medium and high flow stacks, urban/rural approaches, all buildings.

Angled Wind Directions. Due to the limited number of diagonal wind direction trials in this study (only 5 ft [1.52 m] medium flow stacks were studied), it was concluded that insufficient data were available to develop a general equation. Instead, the most conservative F_{VH} results were selected as representative of the diagonal wind direction results. The resulting F_{VH} values were 1.0, 3.6, and 7.8 for respective A_P values of 1.25, 8.0, and 15.0. The trend here is that F_{VH} decreases with increasing A_P, which is the opposite of the trend for the normal wind directions. This result suggests more research is needed to determine a general relationship.

Rooftop Barriers. No general reduction factor relation was evident for the rooftop barrier cases. However, the data showed the following for 5 or 10 ft (1.52 or 3.05 m) stacks and a roof barrier that is 10 ft × 10 ft × 30 ft (3.05 m × 3.05 m × 9.15 m) or greater, oriented perpendicular to the plume direction: (1) the recommended F_{VH} is 1.5 for buildings with A_P of 15, and (2) the recommended reduction factor is 1.0 for buildings with A_P of 8. These conclusions are very restricted, due to the lack of experimental data with varying configurations, and are stated in a manner to produce conservative predictions. A more refined analysis (i.e., wind tunnel simulations) would be required to obtain concentration estimates for cases not covered by this study.

Method to Estimate Concentrations at Hidden Intakes

The concentration at the hidden (sidewall) receptor is calculated as follows:

$$\left(\frac{C}{m}\right)_{SW} = \frac{\left(\frac{C}{m}\right)_{RT}}{F_{VH}F_{SW}} \tag{17}$$

where $(C/m)_{SW}$ is the normalized concentration at the hidden (sidewall) receptor of interest, $(C/m)_{RT}$ is the normalized concentration at downwind rooftop edge, F_{VH} is the visible/hidden reduction factor, and F_{SW} is the sidewall reduction factor. Note that at the top sidewall receptor, F_{SW} is equal to one. The following four-step method is proposed to calculate the hidden air intake concentration.

Step 1—Obtain Input Parameters to Estimate C/m_{RT}. These parameters vary depending on the method used to estimate the rooftop concentration. The input parameters for three possible methods were discussed previously.

Step 2—Determine the Highest $(C/m)_{RT}$. This can be accomplished using ASHRAE (1999) or a Gaussian plume model. The Gaussian plume model could be the one developed by the authors, discussed previously, or EPA models such as ISC (EPA 1995a) or SCREEN3 (EPA 1995b).

Step 3—Determine F_{VH}. This is accomplished by first calculating the values for exhaust flow rate, normalized plan area, and nondimensional stack height. Next, find the appropriate value for F_{VH} in Table 4 for winds normal to the building face or the values listed above for winds diagonal to the building. If the volume flow is above 50,000 cfm (2.36 m^3/s), then Table 4 should be used with caution. Interpolate with caution, tending toward the lower value of F_{VH}, because the patterned areas in the table are already interpolations or extrapolations of observed data. Alternatively, F_{VH} can be calculated by using A_i values from Table 3 of Equation 13, using the values in the right-most column for volume flows ≥ 5000 cfm (2.36 m^3/s).

Step 4—Determine F_{SW}. Determine F_{SW} by using Figures 4a and 4b for bottom and mid-wall locations, respectively. Note that F_{SW} = 1.0 for two cases: (1) for top sidewall receptors by definition and (2) for R > 118 ft (36 m). Alternatively, Fsw can be calculated using Equation 16 and the A_i values listed in the text of the "Sidewall Reduction Factors" section, above. Note that in the equation, Δz is the vertical distance, always positive, between the roof and the receptor.

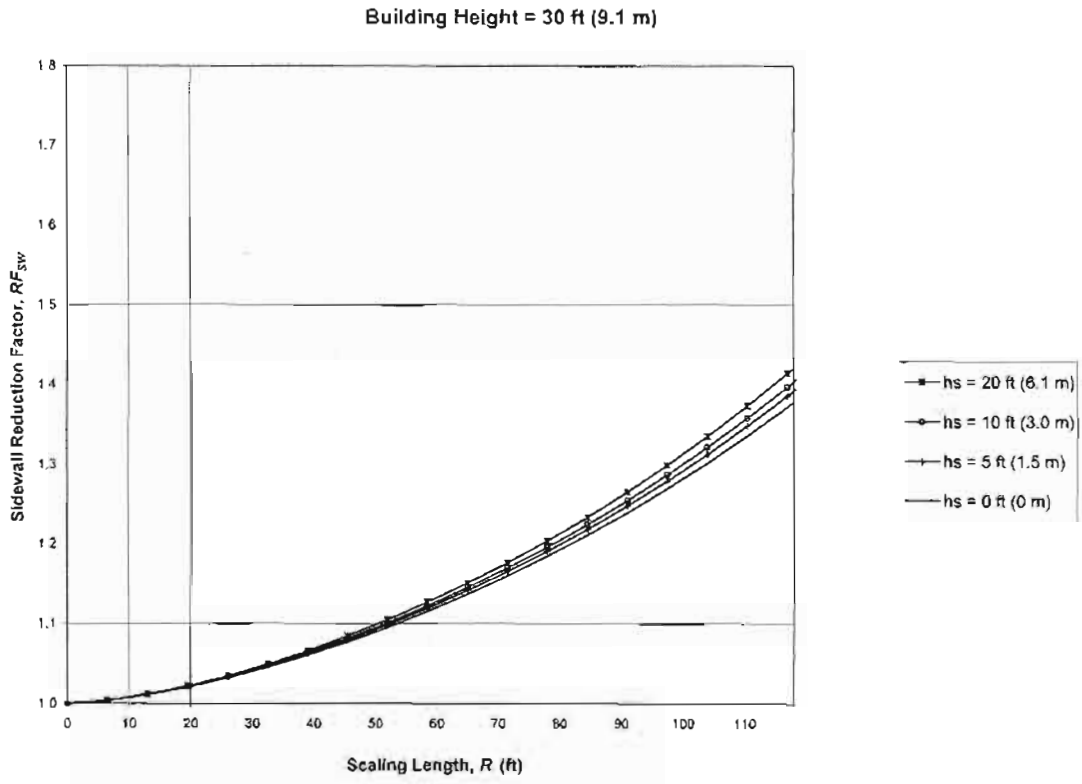

Figure 3 Predicted sidewall reduction factor versus scaling length for various stack heights on a 30 ft (9.1 m) building.

Evaluation of Method

A comparison of the three methods previously described for predicting the concentration at visible and hidden intakes (standard Gaussian, modified Gaussian, and ASHRAE) was conducted to determine which method provides the best agreement with observations and to compare their relative benefits. Details of the evaluation and discussion of the results are presented in Appendix A.

Visible Intake Concentration Estimates. In general, any of the three methods could be used with confidence that prediction of concentrations at the visible intake location will be accurate within a factor of two, with the following limitations:

- The standard Gaussian method should be used with caution for configurations where it is questionable whether the plume will reach the receptor (e.g., medium to tall stacks and/or short distances). It should not be used for buildings with large frontal area (R > 118 ft), due to the possibility that the plume spread parameters won't adequately represent the turbulence condition above the building and may underpredict the concentration at the rooftop edge receptor.
- The modified Gaussian method should not be used when it is likely that the exhaust flow will be captured in the rooftop recirculation cavity, for example, short upwind or center stacks with low or medium volume flow.

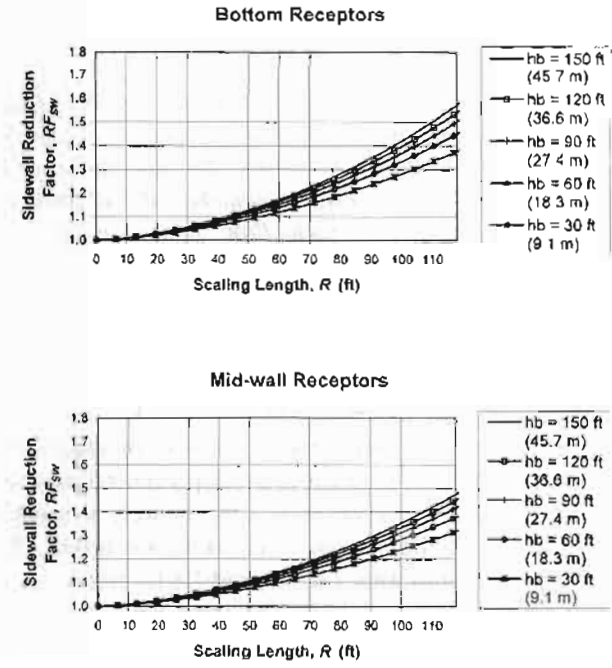

Figure 4 Predicted sidewall reduction factor versus scaling length for various building heights: (a) bottom receptor; (b) mid-wall receptor.

- The ASHRAE method is the most universally accurate and requires the least information, but it should not be used for buildings with large frontal area ($R > 118$ ft).

Hidden Intake Concentration Estimates. Overall, the ASHRAE method is proven to be quite acceptable for estimates of hidden intake concentration, with accurate, yet conservative, predictions and minimal design information requirements. However, it can severely underpredict when $R >$ 118 ft (36 m). In these cases, the modified Gaussian method is recommended if the design closely matches one of those presented in Table 4 and Figure 4. If this is not appropriate, then a wind tunnel simulation should be conducted.

CONCLUSIONS

The study found that placing air intakes on the building sidewalls resulted in widely ranging concentration reductions from the maximum building edge rooftop concentration. The reduction factors depended upon building shape, wind direction, exhaust flow rate, stack height, and vertical distance from the roof to the receptor.

Building Shape and Wind Direction

- For normal wind directions (i.e., flow direction normal to any building face), concentration reduction factors from the edge of the roof to the top sidewall receptor, F_{VH}, tended to decrease with increasing normalized building plan area (A_P). Typical concentration reductions were 2 to 5 for short buildings with short stacks ($h_s / R \leq 0.2$) and 4 to 13 ($h_s / R \leq 0.06$) for tall buildings with short stacks.
- For diagonal wind directions, F_{VH} tended to increase with increasing A_P. More research is suggested for diagonal wind directions.
- For the short building ($A_P = 15.0$), reduction factors at the bottom of the sidewall were approximately the same as at the top of the sidewall.
- For the medium building ($A_P = 8.0$), reduction factors at the bottom of the sidewall were about 1.5 times those at the top of the sidewall.
- For the large building ($A_P = 1.25$), the reduction factors varied from 1.0 to 5.6 times those at the top of the sidewall.

Stack Height

- For normal wind directions, F_{VH} tended to decrease with increasing stack height.
- For diagonal wind directions, only one stack height was tested, but a trend similar to that observed for the normal wind directions is expected.
- The results indicate that when the stack is taller than about $0.5R$, the reduction factors on the sidewall are minimal, suggesting the plume most likely clears the building roof entirely.

Exhaust Flow Rate

- For normal wind directions, reduction factors tended to be the greatest for the low exhaust flow and about the same for the medium and high exhaust flows.
- For diagonal wind directions, only one exhaust flow was tested, but a trend of increasing F_{VH} with decreasing exhaust flow is expected.

Approach Surface Roughness

- The results showed less than 20% variation in reduction factor for a rural or urban approach.

Stack Distance or Plume Size

- For small and medium buildings at normal wind directions, stack location did not tend to affect F_{VH}.
- For large buildings that have large distances along the roof, F_{VH} tended to increase as stack location moved downwind.

Roof Barriers

- The reduction factor for a roof barrier tends to decrease as the relative height of the barrier to the height of the building decreases.

SUMMARY

A method was developed for estimating the concentration on the building sidewall based on the downwind rooftop edge concentration. The method makes use of the existing equations in Chapter 43 of the *1999 ASHRAE Handbook—HVAC Applications* (ASHRAE 1999) to estimate rooftop concentrations and then uses simple algebraic relations or tables and charts to arrive at sidewall concentration estimates. The method was tested against the wind tunnel observations and was found to provide generally accurate and conservative results. Some form of this method is likely to be included in the next edition of the handbook.

Overall, the study has shown what designers suspected: placing air intakes on building sidewalls is beneficial when the stacks are on the roof. Significant concentration reductions were found when air intakes are placed right below the building roof edge on the building sidewall. The farther down the building sidewall the air intake is placed, the larger the reduction. However, the largest relative reduction between a visible and hidden intake is achieved by just moving the intake a few feet from the edge of the building roof to a point just around the corner on the building sidewall.

ACKNOWLEDGMENTS

The authors would like to thank the members of ASHRAE Technical Committee 4.3, Ventilation Requirements and Infiltration, for sponsoring this work.

NOMENCLATURE

A_e = stack exit area
A_i = empirical constants
A_P = normalized plan area
B_1 = distance dilution parameter
B_L = the larger of the building upwind face height or width
B_s = the smaller of the building upwind face height or width
C = pollutant concentration
C/m = normalized concentration
$(C/m)_{RT}$ = normalized concentration at downwind rooftop edge
$(C/m)_{SW}$ = normalized concentration at the sidewall receptor of interest
C_{top} = concentration at top sidewall receptor
C_{bot} = concentration at bottom sidewall receptor
d = stack diameter
F_{SW} = concentration reduction factor for intakes at various heights along a building sidewall (sidewall reduction factor)
F_{VH} = concentration reduction factor between visible and top hidden intakes (visible/hidden reduction factor)
h_b = building height
h_s = stack height above the roof, receptor, or ground level as appropriate
(h_s/R) = normalized stack height
I_{xs} = longitudinal turbulence intensity at the stack location
$I_{xs,ap}$ = longitudinal turbulence intensity in the approach flow at stack height
I_{ys} = lateral turbulence intensity at the stack location
$I_{ys,ap}$ = lateral turbulence intensity in the approach flow at stack height
I_{zs} = vertical turbulence intensity at the stack location
$I_{zs,ap}$ = vertical turbulence intensity in the approach flow at stack height
$(I_y/I_{x,ap})_s$ = factor for a specific stack/building configuration to relate the approach longitudinal turbulence intensity to the lateral turbulence intensity at the stack location
$(I_z/I_{x,ap})_s$ = factor for a specific stack/building configuration to relate the approach longitudinal turbulence intensity to the vertical turbulence intensity at the stack location
m = pollutant mass emission rate
n_{anem} = power law exponent at the anemometer
n_{site} = power law exponent at the building site
R = ASHRAE (1999) scaling length
S = stretched-string distance
T_a = ambient temperature
T_s = exhaust gas temperature
U_{anem} = mean wind speed at the anemometer height, z_{anem}
U_h = mean wind speed at stack top
$U_{h,i}$ = mean velocity in the approach flow at stack height
$U_h/U_{h,ap}$ = factor for a specific stack/building configuration to relate the approach wind speed to wind speed at the stack location
V_e/U_h = velocity ratio
x = downwind distance of the receptor location
z_∞ = free stream height
z_{anem} = anemometer height
z_s = stack height above ground level
z_{ref} = reference height

Greek

β_j = entrainment dilution parameter
Δh_T = net effective rise of the plume centerline above the stack top
Δz = vertical distance from roof to receptor
σ_y = standard deviation of plume concentration distribution in the crosswind direction at downwind distance x
σ_{y0} = initial lateral plume dispersion
σ_{yt} = lateral plume dispersion due to ambient turbulence
σ_z = standard deviation of plume concentration distribution in the vertical direction at downwind distance x
σ_{z0} = initial vertical plume dispersion
σ_{zt} = vertical plume dispersion due to ambient turbulence

REFERENCES

ASHRAE. 1999. Building air intake and exhaust design. *1999 ASHRAE Handbook—HVAC Applications*. Atlanta: American Society of Heating, Refrigerating and Air-Conditioning Engineers, Inc.

Briggs, G.A. 1969. Plume rise. USAEC Critical Review Series, TID-25075, Clearinghouse for Federal Scientific and Technical Information.

Briggs, G.A. 1975. Plume rise predictions. Lectures on Air Pollution and Environmental Impact Analyses. American Meteorological Society.

Cimorelli, A.J., S.G. Perry, A. Venkatram, J.C. Weil, R.J. Paine, R.B. Wilson, R.F. Lee, and W.D. Peters. 1998. AERMOD Description of Model Formulation, draft document U.S. EPA, Office of Air Quality Planning and Standards. Research Triangle Park, North Carolina, December 15.

EPA. 1995a. SCREEN3 user's guide. EPA-454/B-95-004. U.S. Environmental Protection Agency, Research Triangle Park, North Carolina (NTIS No. PB 95-222766).

EPA. 1995b. User's guide for the industrial source complex (ISC3) dispersion models: Volume II—Description of model algorithms. U.S. Environmental Protection Agency, Office of Air Quality Planning and Standards;

Emissions, Monitoring, and Analysis Division, Research Triangle Park, North Carolina. Report No. EPA-454/B-95-004. September.

Halitsky, J. 1963. Gas diffusion near buildings. *ASHRAE Transactions*, Vol. 69, pp. 464-484.

Hanna, S.R., and D.W. Heinhold. 1985. Development and application of a simple method for evaluating air quality models. American Petroleum Institute Publication No. 4409. January.

Hosker, R.P., Jr. 1985. Flow around isolated structures and building clusters: A review. *ASHRAE Transactions* 91(2B): 1671-1692.

Huber, A.H. 1978. Determination of good engineering practice stack height. 71st Annual Meeting of the APCA, June 25-30.

Huber, A.H. 1988a. Performance of a Gaussian model for centerline concentrations in the wake of buildings. *Atmospheric Environment* 22(6): 1039-1050.

Huber, A.H. 1988b. Video images of smoke dispersion in the near wake of a model building. Part II. Cross-stream distribution. *Journal of Wind Engineering and Industrial Aerodynamics*, Vol. 32, pp. 263-284.

Huber, A.H. 1989. The influence of building width and orientation on plume dispersion in the wake of a building. Report to the U.S. EPA Atmospheric Research and Exposure Assessment Laboratory. U.S. EPA, Research Triangle Park, North Carolina.

Li, W.W., and R.N. Meroney. 1983. Gas dispersion near a cubical model building, Part I: Mean concentration measurements. *Journal of Wind Engineering and Industrial Aerodynamics*, Vol. 12, pp. 15-33.

Petersen, R.L., J.J. Carter, and M.A. Ratcliff. 1997. The influence of architectural screens on exhaust dilution. Final Report, ASHRAE 805-TRP.

Petersen, R.L., and J.W. LeCompte. 2002. Exhaust contamination of hidden versus visible air intakes. Final Report, ASHRAE 1168-TRP.

Snyder, W.H. 1981. Guideline for fluid modeling of atmospheric diffusion. U.S. EPA, Environmental Sciences Research Laboratory, Office of Research and Development, Research Triangle Park, North Carolina, Report No. EPA-600/8-81-009.

Turner, D.B. 1994. *Workbook of Atmospheric Dispersion Estimates: An Introduction to Dispersion Modeling*, 2nd ed. Boca Raton: Lewis Publishers.

Wilson, D.J. 1976. Contamination of air intakes from roof exhaust vents. *ASHRAE Transactions* 82(1): 1024-1038.

Wilson, D.J. 1977a. Effect of vent stack height and exit velocity on exhaust gas dilution. *ASHRAE Transactions*, 83(1): 157-166.

Wilson, D.J. 1977b. Dilution of exhaust gases from building surface vents. *ASHRAE Transactions* 83(1): 168-176.

Wilson, D.J., I.C. Fabris, J. Chen, and M.Y. Ackerman. 1998. Adjacent building effects on laboratory fume hood exhaust stack design. Final Report, ASHRAE Research Project 897. January.

APPENDIX A

A comparison of the three methods previously described for predicting the concentration at visible and hidden intakes (standard Gaussian, modified Gaussian, and ASHRAE) was conducted to determine which method provides the best agreement with observations. The performance of the methods was evaluated with respect to how each (1) predicted concentrations conservatively (little or no underprediction) and (2) limited scatter and overprediction. The methods were evaluated using two statistical quantities described in Hanna and Heinhold (1985) that are frequently used to evaluate analytical model performance: normalized mean square error (NMSE) and normalized bias (NB).

The comparisons were conducted using a concentration framework in which a high value is conservative, i.e., a greater quantity of the emitted pollutant is present. If a dilution framework was used, a low dilution value would be conservative.

Visible Intake Concentration Estimates. Table A-1 lists the NMSE and NB resulting from comparison of predicted and observed rooftop concentrations. It is evident that the modified Gaussian and ASHRAE methods produced the best overall results. The two methods produced comparable values for NMSE. The modified Gaussian method produced a lower NB, while the ASHRAE method produced a more conservative estimate (characterized by the larger negative NB value). Note that the standard Gaussian method also resulted in a negative average NB, but the average NMSE was significantly greater than that for the other two methods.

Table A-1. Normalized Mean Square Error (NMSE) and Normalized Bias (NB) Using Three Methods to Estimate Visible Intake Concentrations

	Method					
	Standard Gaussian		Modified Gaussian		ASHRAE	
Building Number	NMSE	NB	NMSE	NB	NMSE	NB
1	2.01	-0.83	0.51	0.07	0.45	-0.34
2	1.24	-0.70	0.48	0.21	0.47	-0.51
3	12.73	-3.31	0.56	-0.39	1.44	-0.57
Overall	5.76	-1.44	0.52	-0.01	0.69	-0.46

Table A-2. Normalized Mean Square Error (NMSE) and Normalized Bias (NB) Using Three Methods to Estimate Sidewall Intake Concentrations

Top Sidewall Intake						
	Method					
	Standard Gaussian		Modified Gaussian		ASHRAE	
Building Number	NMSE	NB	NMSE	NB	NMSE	NB
1	1.66	-0.87	0.34	-0.07	0.73	-0.53
2	1.07	-0.60	0.41	0.21	0.40	-0.48
3	18.35	-4.99	0.86	-0.76	1.21	-0.86
Overall	3.8	-1.31	0.47	-0.07	0.85	-0.55
Bottom Sidewall Intake						
	Method					
	Standard Gaussian		Modified Gaussian		ASHRAE	
Building Number	NMSE	NB	NMSE	NB	NMSE	NB
1	1.69	-0.92	0.29	-0.10	0.80	-0.57
2	1.01	-0.60	0.32	0.20	0.46	-0.48
3	17.00	-4.94	1.05	-0.80	1.72	-0.93
Overall	3.27	-1.24	0.45	-0.09	1.08	-0.58

Designs based strictly on modified Gaussian predictions are likely to be accurate, while designs based on standard Gaussian and ASHRAE predictions will, on average, tend to be conservative. That is, they will require higher stack heights and/or volume flows to meet the required design concentration.

Hidden Intake Concentration Estimates. Table A-2 lists the NMSE and NB resulting from comparison of predicted and observed sidewall concentrations at the top and bottom sidewall receptors, respectively. Since the same empirical factors, F_{VH} and F_{SH}, were used to adjust the rooftop concentrations to predict the sidewall (hidden) concentrations, predictions for each method follow similar trends as those for the visible intakes for the same method. Effectively, the configurations where each of the methods is weak in predicting the visible intake concentration should also be avoided in predicting hidden intake concentrations.

The standard Gaussian method again had high NMSE values for Building 3 hidden concentration predictions, markedly increased from the visible intake results shown in Table A-1. However, this method again predicted conservatively in most cases, except for medium to tall stacks and short distances. For many cases, the method overpredicted considerably, sometimes by more than an order of magnitude.

The modified Gaussian method again tended to predict accurately and centrally, rather than conservatively, having the lowest absolute values of NMSE and NB in Table A-2. In almost all cases, the underprediction was minor (less than a factor of two), with virtually no underprediction for middle and bottom sidewall receptor locations.

The ASHRAE method again predicted fairly accurately and conservatively, with NMSE values roughly twice those of the modified Gaussian method. The overpredictions increased in magnitude (occasionally by an order of magnitude) due to the conservative bias in the results from the visible intake calculations, although these cases had such low C/m values as to be inconsequential.

DISCUSSION

Gideon Rozen, Founder, HRVAC Consulting Engineering, Tel Moud, Israel: Presentation very well prepared and clear. Visit worthwhile.

Ron Petersen: Thank you for your interest in our presentation.